Role of Metals in the Biological Activity of *Clostridium botulinum* Neurotoxins[†,‡]

Subramaniam Eswaramoorthy,[§] Desigan Kumaran,[§] James Keller,[||] and Subramanyam Swaminathan*[,§]

Biology Department, Brookhaven National Laboratory, Upton, New York 11973, and Laboratory of Bacterial Toxins, Food and Drug Administration, Bethesda, Maryland 20892

Received October 13, 2003; Revised Manuscript Received December 22, 2003

ABSTRACT: *Clostridium botulinum* neurotoxins are the most potent toxins to humans and cause paralysis by blocking neurotransmitter release at the presynaptic nerve terminals. The toxicity involves four steps, viz., binding to neuronal cells, internalization, translocation, and catalytic activity. While the catalytic activity is a zinc endopeptidase activity on the SNARE complex proteins, the translocation is believed to be a pH-dependent process allowing the translocation domain to change its conformation to penetrate the endosomal membrane. Here, we report the crystal structures of botulinum neurotoxin type B at various pHs and of an apo form of the neurotoxin, and discuss the role of metal ions and the effect of pH variation in the biological activity. Except for the perturbation of a few side chains, the conformation of the catalytic domain is unchanged in the zinc-depleted apotoxin, suggesting that zinc's role is catalytic. We have also identified two calcium ions in the molecule and present biochemical evidence to show that they play a role in the translocation of the light chain through the membrane.

Clostridium neurotoxins comprise the seven antigenically distinct neurotoxins (BoNT/A-G)[1] produced by *Clostridium botulinum* and tetanus neurotoxin produced by *Clostridium tetani*. Active neurotoxins are two-chain molecules, a heavy chain (HC, 100 kDa) and a light chain (LC, 50 kDa) held together by a disulfide bond (*1*). Botulinum neurotoxins act on the peripheral nervous system and inhibit the release of acetylcholine at the neuromuscular junction (*2*). Tetanus toxin acts on the central nervous system and inhibits the release of glycine and γ-aminobutyric acid (*3*). They all share significant sequence homology and functional similarity and are expected to have similar three-dimensional structures. *C. botulinum* neurotoxins follow a four-step process of toxicity (*4*−*6*). The C-terminal half of the HC binds to the presynaptic membrane via gangliosides and to a second protein receptor, and then the toxin is internalized by receptor-mediated endocytosis. The N-terminal half of the HC helps in translocating the LC into the cytosol where the latter cleaves one of the three target proteins at specific peptide bonds, thus inhibiting formation of the SNARE complex, which is necessary for docking and fusion of vesicles to membranes. This in turn blocks the release of neurotransmitters and causes flaccid (botulinum toxins) or spastic paralysis (tetanus toxin). The LCs of all neurotoxins contain a conserved zinc-binding motif (HExxH+E), and accordingly, at least one zinc atom is present per molecule (*7*). The catalytic activity is a zinc endopeptidase activity, and therefore, the presence of zinc is required for activity. Though they have similar functions and sequences, the target protein and the scissile bonds are specific for each neurotoxin. BoNT/A, -E, and -C1 cleave synaptosomal-associated protein (SNAP-25) at different peptide bonds. BoNT/B, -D, -F, and -G and tetanus toxin cleave vesicle-associated membrane protein (VAMP). BoNT/C also cleaves syntaxin (*7*−*15*).

The role of zinc in *Clostridium* neurotoxins has been studied extensively by biochemical and biophysical methods. A zinc atom is present in many proteins, and its role is to maintain the structural integrity, the functional integrity, or both (*16*−*18*). There are conflicting opinions about the role of zinc in *Clostridium* neurotoxins. It has been shown to be functional in the case of BoNT/B and tetanus toxin since the catalytic activity that was lost upon the removal of zinc was regained when it was introduced again into the protein, suggesting that there is no structural change when zinc is removed or reintroduced (*7*, *19*, *20*). In the case of intact BoNT/A, the activity could not be restored by reintroducing the zinc atom. This led to the conclusion that while the removal of zinc is reversible, the activity is irreversibly lost presumably due to a change in the tertiary structure (*21*). This was supported by circular dichroism and spectroscopic studies. However, the activity could be restored in the BoNTA light chain, though to a lesser extent (*22*). Simpson et al. (*23*) have recently shown that the role of zinc is only catalytic. However, no X-ray structure of the zinc-depleted protein has been available until now for comparing the apo- and holotoxin conformations directly. Here, we present the

[†] Research supported by the Chemical and Biological Non-proliferation Program (NN20) of the U.S. Department of Energy and the U.S. Army Medical Research Acquisition Activity (Award DAMD17-02-2-0011) under DOE Prime Contract DE-AC02-98CH10886 with Brookhaven National Laboratory.

[‡] The coordinates for the structures have been deposited in the Protein Data Bank as entries 1S0B, 1S0C, 1S0D, 1S0E, 1S0F, and 1S0G.

* To whom correspondence should be addressed. E-mail: swami@bnl.gov. Telephone: (631) 344-3187. Fax: (631) 344-3407.

[§] Brookhaven National Laboratory.

[||] Food and Drug Administration.

[1] Abbreviations: BoNT, botulinum neurotoxin; HC, heavy chain; LC, light chain; SNARE, soluble NSF accessory protein receptors; SNAP-25, synaptosome-associated protein of 25 kDa; VAMP, vesicle-associated membrane protein; DTT, dithiothreitol; EDTA, ethylenediaminetetraacetate; TPEN, *N*,*N*,*N*′,*N*′-tetrakis(2-pyridylmethyl)ethylenediamine; PMSF, phenylmethanesulfonyl fluoride; BAPTA, 1,2-bis(2-aminophenoxy)ethane-*N*,*N*,*N*′,*N*′-tetraacetic acid; HEPES, *N*-(2-hydroxyethyl)piperazine-*N*′-2-ethanesulfonic acid.

10.1021/bi035844k CCC: $27.50
Published on Web 02/06/2004

first three-dimensional structure of an apo *Clostridium* neurotoxin determined by X-ray diffraction.

The process of translocation of the LC into the cytosol is still a puzzle. The translocation domain probably changes its conformation due to the pH change in the endosome which allows it to insert itself into the endosomal membrane and translocate the LC into the cytosol (*5*, *24*). We have determined the crystal structure of BoNT/B at various pH values ranging from 4 to 7 and show that there is no conformational change at the putative transmembrane region, at least in the crystal structures. There may be other factors, yet unknown, involved in the translocation (*25*). We have identified two calcium ions bound to the toxin molecule which play a role in the translocation of the catalytic domain.

In this report, we present the results from the crystal structure analysis of the apotoxin and BoNT/B crystallized at various pHs and also provide biochemical evidence which shows that calcium is required for translocation of the neurotoxin into the cytosol.

EXPERIMENTAL PROCEDURES

Reagents. Trypsin, soybean trypsin inhibitor, *N*,*N*,*N*′,*N*′-tetrakis(2-pyridylmethyl)ethylenediamine (TPEN), phenylmethanesulfonyl fluoride (PMSF), 1,2-bis(2-aminophenoxy)-ethane-*N*,*N*,*N*′,*N*′-tetraacetic acid (BAPTA), the membrane-permeable BAPTA-AM, and dithiothreitol were from Sigma Chemical Co. (St. Louis, MO). SDS−PAGE and Western blotting supplies were from Bio-Rad (Hercules, CA).

Toxin Preparation. In the case of cell culture experiments, BoNT/A and -B were obtained from Wako Chemicals (Richmond, VA). According to the manufacturer's instructions, BoNT/B [1 mg/mL in 0.2 M NaCl and 50 mM NaOAc (pH 6.0)] was treated with trypsin (0.2 mg/mL) at 37 °C for 0.5 h. Trypsin was inhibited by addition of soybean trypsin inhibitor (0.5 mg/mL). Both serotypes were aliquoted and frozen at −20 °C. The clone, LC-pET30 with two six-histidine tags and one S-tag, for the BoNT/A light chain was a gift from R. Balhorn. It was expressed and purified in Swaminathan's laboratory as described previously (*26*). BoNT/B for crystallization was purchased from Metabiologics (Madison, WI).

Testing BoNT Action. Cultured spinal cord neurons were prepared from E12 mouse embryos and plated onto 35 mm dishes at a density of 1×10^6 cells. Cultures were maintained in MEM medium containing 5% horse serum (*27*−*29*) and fed with half-medium changes twice per week. Because Ca^{2+} is required for many cell functions, the toxin (BoNT/A and -B at 0.5 and 2 nM, respectively) was applied to cells in the presence of 2 mM Ca^{2+} to allow normal toxin binding and endocytosis. Four minutes after the toxin had been added, cultures were washed to remove unbound toxin and then were incubated for 2.5 h at 37 °C. The Ca^{2+}-specific chelator BAPTA-AM was prepared as a 50 mM stock solution in DMSO. This was diluted into Ca^{2+}-free MEM and applied to cultures immediately after toxin washout. The absence of Ca^{2+} in the extracellular medium after toxin application did not alter intracellular BoNT activity. To directly test toxin activity on SNARE substrates, some cultures were lysed using 0.6% Triton, 0.5 mM PMSF, 1 mM DTT, and 25 mM HEPES (pH 7.2). The lysate was incubated on ice for 1 h to allow PMSF to degrade prior to toxin addition. Lysate/toxin mixtures were incubated at room temperature for 3 h.

SDS−PAGE and Western Blot Analysis. We prepared samples from neuronal cultures or lysates for SDS−PAGE by dissolving them in 2% SDS and 0.5% mercaptoethanol and boiling for 4 min. Proteins were separated on 15% acrylamide gels (*30*) and transferred to a PVDF membrane. Western blotting utilized antibodies to SNARE complex proteins: the anti-SNAP-25 antibody was from Sternberger Monoclonals (Lutherville, MD), anti-Synaptobrevin-2 from Synaptic Systems, and anti-syntaxin from Sigma Chemical Co. A secondary antibody was conjugated to horseradish peroxidase and visualized using ECL-Plus chemiluminescent substrate (Amersham Bioscience, Piscataway, NJ). Blot images were obtained by scanning with the STORM 860 fluorescent detector and ImageQuant software (Molecular Dynamics).

Preparation of the Protein for Crystallization. BoNT/B was supplied as a precipitate in 50% ammonium sulfate. This was spun at 5000 rpm in a refrigerated microcentrifuge, and the supernatant was discarded. The precipitate was dissolved in 50 mM HEPES, 100 mM NaCl, and 10 mM dithiothreitol (DTT) at pH 7.0. DTT was used since the BoNT endopeptidase activity is expressed only after the disulfide bond is reduced (*31*). Also, because the protein is supplied as a precipitate in ammonium sulfate, a sulfate ion was found to be present in the catalytic site (*32*). The protein was dialyzed against 100 mM NaCl, 50 mM HEPES, and 10 mM dithiothreitol at pH 7.0 overnight in two steps. Then 80 mM barium acetate was added to the dialysate to remove the sulfate ion bound in the catalytic site and dialyzed twice more. The final dialysis was carried out without barium acetate.

Preparation of the Apoprotein. The protein (1 mg/mL) was prepared as described above, but metal-free HPLC-grade water was used throughout. The protein was then treated with ethylenediaminetetraacetate (EDTA) to a final concentration of 15 mM and incubated for 1 h at 37 °C. This was again extensively dialyzed against 50 mM HEPES, 100 mM NaCl, and 10 mM DTT at pH 7.0 to remove EDTA and the zinc−EDTA complex (*21*).

Crystallization. The crystallization condition for both apo- and holoneurotoxins is as described but under a reducing condition (*33*). In the case of the apoprotein, the reagents were prepared with HPLC-grade water. For the holotoxin, crystallization was carried out at pH 5.0 using appropriate buffer. To determine crystal structures at other pH values, the pH of the mother liquor was slowly titrated with appropriate buffers (sodium citrate for pH <5.5 and HEPES for pH >5.5), allowing enough time (6 h for each change) for the crystals to equilibrate with the mother liquor. The crystals were monitored periodically to check for any physical damage. Crystals were obtained at pH 4.0, 5.0, 5.5, 6.0, and 7.0.

Data Collection. Data were collected at liquid nitrogen temperature at X12C and X25 beamlines of the National Synchrotron Light Source, Brookhaven National Laboratory, with a Brandeis CCD-based B1 or B4 detector. An oscillation range of 1° was used for each data frame, and data corresponding to 200° in ϕ were collected with a crystal to detector distance of 100 mm (200 mm at X25) and a λ of 1.00 Å. Data were reduced with DENZO and SCALEPACK (*34*). Data collection statistics are given in Table 1.

Table 1: Crystal Data and Refinement Statistics[a]

	pH 4.0	pH 5.0	pH 5.5	pH 6.0	pH 7.0	apo
Crystal Data						
resolution (Å)	2.0	2.2	2.2	1.9	2.3	2.6
total no. of reflections	284241	295339	275095	368649	254516	172822
no. of unique reflections	97573	81173	78587	118562	64761	49302
completeness (%)[b]	89.1 (69.4)	99.7 (98.4)	94.3 (74.8)	92.8 (55.4)	89.8 (51.9)	99.7 (97.7)
R_{sym}[c]	0.059 (0.218)	0.079 (0.310)	0.067 (0.397)	0.048 (0.308)	0.084 (0.497)	0.055 (0.166)
Refinement Parameters						
resolution (Å)	50.0−2.0	50.0−2.2	50.0−2.2	50.0−1.9	50.0−2.3	50.0−2.6
no. of reflections	94427	77445	70860	112138	58061	48272
R[d]	0.204	0.204	0.223	0.206	0.226	0.210
R_{free}[e]	0.234	0.240	0.273	0.235	0.287	0.265
no. of atoms						
protein	10587	10587	10587	10587	10430	10594
Zn^{2+}	−	1	1	1	1	−
Ca^{2+}	2	2	2	2	2	−
no. of water molecules	1034	582	547	857	428	379
rmsd						
bond lengths (Å)	0.006	0.006	0.007	0.006	0.007	0.007
bond angles (deg)	1.21	1.23	1.26	1.21	1.28	1.27
% residues in the most favored region of the $\phi-\psi$ plot[f]	88.4 (11.0)	88.1 (11.0)	87.6 (11.5)	88.1 (11.2)	83.2 (15.4)	86.5 (12.7)

[a] Cell parameters at pH 6: $a = 76.05$ Å, $b = 122.91$ Å, $c = 95.43$ Å, and $\beta = 113.1°$. Cell parameters for other pHs and for the apotoxin agree within experimental error. [b] Values for the outermost shells are given in parentheses. [c] $R_{sym} = \sum_h\sum_i|I_i(h) - \langle I(h)\rangle|/\sum_h\sum_i|I_i(h)|$, where $I_i(h)$ is the intensity measurement for reflection h and $\langle I(h)\rangle$ is the mean intensity for this reflection. [d] $R = \sum_i||F_{i,obs}| - k|F_{i,cal}||/\sum_i|F_{i,obs}|$. [e] Approximately 2% of the total reflections were used for R_{free} calculations. [f] Percentage of residues in the additional allowed region given in parentheses.

FIGURE 1: SigmaA-weighted $2F_o - F_c$ map at the active site of the apotoxin. Contours are drawn at the 1σ level. There is no residual density corresponding to the original zinc site. The residual density close to the zinc site is due to water molecules. The coordination with Glu267 is lost. There is a water molecule near the original zinc site which may be disordered. This figure was prepared with Molscript (*52*).

Structure Determination. Initial model coordinates were obtained from Protein Data Bank entry 1epw. After initial rigid body refinement, the structures were refined with CNS (*35*). Adjustments of the original model were done with O (*36*) against a composite omit map to remove model bias. The protein model is complete except for residues 440−442, which are in the proteolytic site. In the case of the apoprotein, the sigmaA-weighted $2F_o - F_c$ map showed no density at the zinc site, confirming the absence of zinc (Figure 1) (*37*). The model was further refined with water molecules and metals (if present) included. Refinement statistics are included in Table 1. Structures were validated with PROCHECK (*38*), and the percentages of residues in the most favored region of the Ramachandran plot are given in Table 1.

RESULTS AND DISCUSSION

Structure of BoNT/B at pH 4, 5, 5.5, 6, and 7. The crystal structure of BoNT/B was determined under various (pH) conditions. A Ribbons representation of the molecule is given in Figure 3. The BoNT molecule consists of three functional domains which are the binding, translocation, and catalytic domains (left to right in Figure 3). The translocation domain consists mainly of two long helices, and the catalytic domain contains a zinc ion. While the binding domain is presumably invariant to pH variation, the translocation domain is supposed to undergo conformational variation to expose the hydrophobic residues to the membrane bilayer to allow channel formation for the translocation of the LC into the cytosol. The size of the pore formed by the BoNT/B HC has been estimated to be ∼8−15 Å (*25*, *39*), and it is not clear how a 50 kDa domain could escape through it without completely unfolding. It is possible that the light chain completely unfolds at low pH, threads through the pore, and then refolds in the cytosol before attacking its target (*40*). However, there may be other factors involved in the change of conformation. This study is focused on only the effect of pH variation on the conformation of the protein.

Conformation of the Translocation Domain versus pH. Theoretical predictions about the transmembrane region based on hydropathy analysis concluded that the region of residues 637−668 for BoNT/B would be the transmembrane region and could adopt a helical conformation (*41*). However, in the structural analysis of BoNT/B carried out at pH 6.0, this region is not all helical. While residues 638−645 adopt a helical conformation and are in the middle of the molecule, the rest is in an extended conformation. This is similar to the BoNT/A structure which was determined at pH 7.0 (*42*). In BoNT/A, it is suggested that two histidines in the translocation domain (residues 551 and 560) might titrate during the reduction of the pH in the endosome and help in changing the conformation. However, no histidine is present in the translocation domain of BoNT/B to induce conformational change by the same mechanism. This prompted us to determine the structure at lower pH values. Figure 4 shows the superposition of the putative transmembrane region at various pHs. There is no change in the conformation in this

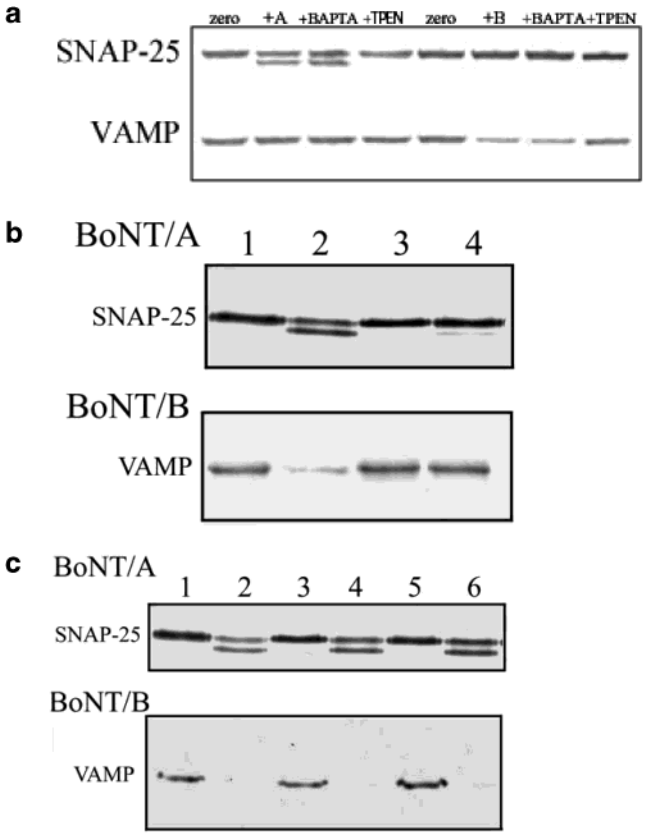

FIGURE 2: (a) Neuronal lysate treated with BoNT and chelators. Lysates were prepared as described in Experimental Procedures and treated with 0.1 mM BAPTA or TPEN as indicated. Reactions were initiated by addition of BoNT/A (10 nM) or BoNT/B (20 nM) light chains and then were stopped 3 h later. Densitometric analysis shows that each toxin cleaved approximately half of the SNARE protein substrate. BAPTA had no noticeable effect, whereas TPEN completely inhibited both, indicating that BAPTA could not chelate Zn^{2+} from the toxin light chains. (b) Living neurons treated with BoNT and chelators. Neuronal cultures were treated with BoNT/A (0.5 nM) or BoNT/B (2 nM). Some cultures were simultaneously treated with BAPTA-AM (80 μM) or TPEN (20 μM): lane 1, untreated; lane 2, BoNT only; lane 3, BAPTA-AM; and lane 4, TPEN. Western blot results show that both chelators inhibit intracellular BoNT activity. (c) Restoration of intracellular BoNT activity following chelator inhibition. Cultures were treated with BoNT as described for panel b except in some cases excess Ca^{2+} or Zn^{2+} was added to cultures: lane 1, untreated; lane 2, BoNT only; lane 3, BoNT and BAPTA-AM; lane 4, BoNT, BAPTA-AM, and 0.1 mM Ca^{2+}; lane 5, BoNT and TPEN; and lane 6, BoNT, TPEN, and 0.1 mM Zn^{2+}. Toxin inhibition by BAPTA-AM is reversed by free Ca^{2+}. Since BAPTA does not inhibit the catalytic activity of BoNT (a), Ca^{2+} probably has a direct role in entry of the toxin into the neuronal cytosol.

region as the pH of the crystal is varied. Though it takes an extended conformation, there is a slight left-handed twist which might suggest an unstable conformation prone to changing readily. We have even titrated the pH to as low as 3.2 (data not presented) and found no change in the conformation. However, it has been suggested that the pH of the endosome need not go below pH 5.0 for translocation of the LC (*25*). It is suggested that the HC−LC complex ingrained in the membrane acts like a chaperone.

The above results raise two questions. (1) Could a change in conformation due to pH be studied by crystal structure determination where packing forces of the crystal lattice might play a major role? Such studies have been carried out. Bullogh et al. (*43*) have shown that a peptide region changes

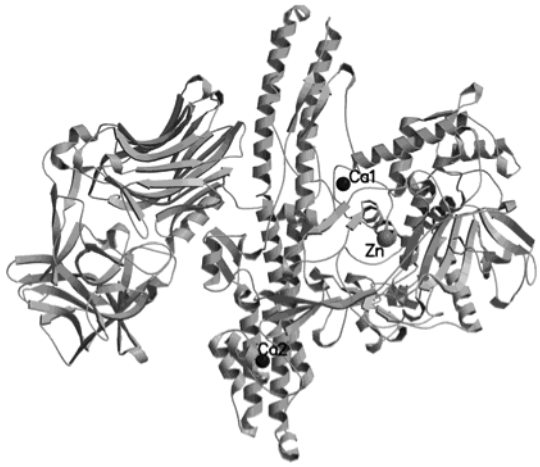

FIGURE 3: Ribbons representation of BoNT/B at pH 6.0. The three metal ions are shown as sphere models, zinc in gray and calcium in black. This figure was prepared with Molscript (*52*).

FIGURE 4: Putative transmembrane region of botulinum neurotoxin B. The α-C trace from structures determined at pH 4.0 (black) and 7.0 (gray) are superimposed, and no major change in conformation is seen. Conformations of this region at other pH values are similar and closer to that at pH 4.0.

its conformation drastically by determining the structures at two vastly different pHs. (2) If it is not the pH, what is responsible for the presumed change in conformation? This study cannot answer that question but can only show that something more than a reduction of the pH is required. Further studies such as the effect of lipids, phosphorylation of toxins, etc., need to be pursued.

Effect of pH on the Catalytic Domain and the Active Site Zinc. Li et al. (*44*) have reported that the zinc ion stays bound to the protein at a pH as low as 4.7. In our structure determination, we monitored the change in the overall conformation of the light chain, the presence of zinc, and specific changes in side chain conformations especially near the active site. As the pH is decreased from pH 6 to 4.0, it is found that the zinc ion gradually becomes disordered (as judged by the thermal factor) and finally is removed altogether. The thermal factor steadily increases compared to the average *B* factor of the protein atoms. Also, the thermal

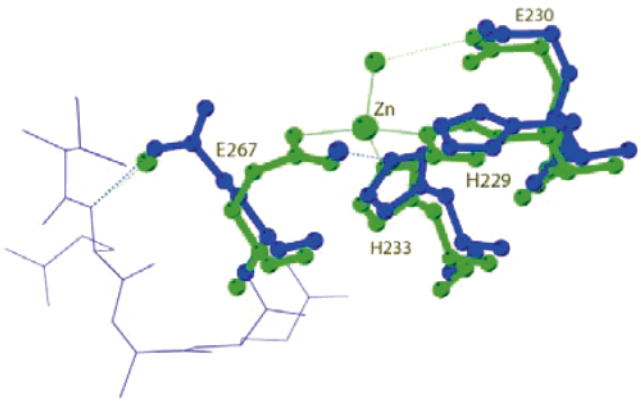

FIGURE 5: Active site of botulinum neurotoxin at pH 6.0 (green) and 4.0 (blue). At pH 6.0 and 7.0 (not shown), the side chain carboxylate oxygen coordinates with zinc. At pH 4.0, this coordination is lost and it takes a different rotamer position making a hydrogen bond with Gln264 (shown with a dashed line) and replaces a water molecule present at pH 6.0 (shown in green). Interestingly, a water molecule (shown in blue) replaces one of the original carboxylate oxygens. At pH 5.5, the side chain of Glu267 takes two discrete orientations. Also, at pH <5.0, the nucleophilic water is not seen in the electron density map.

factors of the terminal atoms of Glu267 increase, and the side chain becomes disordered. At pH 5.5, the side chain has two disordered positions. The position with the higher occupancy still maintains coordination with the zinc ion, while in the second orientation, the carboxylate group makes a hydrogen bond with the main chain nitrogen of Gln264. At pH 5.0, the side chain of Glu267 takes a completely new rotamer position and the coordination to zinc is lost and corresponds to the second disordered position at pH 5.5. Though the thermal factor of zinc increases, electron density persists for the zinc atom, in agreement with the published results (*44*). However, at pH 4.0 and 3.2, Glu267 takes the new rotamer position and there is no electron density for the zinc ion, suggesting that it has been removed completely. In structures at pH <5.0, the nucleophilic water is not present, whereas it is intact (though slightly moved) in structures at pH >5.0 (Figure 5). In all cases, there is no change in the overall conformation and the helical content remains constant contrary to results from biophysical studies which may be due to the difference in solid and solution states or the experimental conditions that are used.

Belt Region versus pH Variation. The main difference between the crystal structures of BoNT/A and BoNT/B (amino acids 481−530) is in the conformation of the belt region with respect to the active site. While the active site is shielded by the belt region in BoNT/A, it is almost completely open to the solvent region in BoNT/B. This difference was thought to be due to the difference in crystallization conditions (BoNT/A at pH 7 and BoNT/B at pH 6). While the zinc coordination remains the same as in the case of the pH 6.0 structure, there is no visible movement of the belt region, suggesting the difference may be real and serotype-specific (Figure 6). This will be confirmed only when structures of other serotypes become available.

Structure of Apo-BoNT/B. The crystal structure of BoNT/B crystallized after treatment with EDTA has been determined to 2.6 Å resolution. The apo-BoNT/B molecule closely resembles those at pH 4 and 3.2. There is no major change in the tertiary structure, and the rmsd is 0.813 Å when compared to the structure at pH 6 for 1270 α-C atoms. The Glu267 side chain takes a new rotamer position as at pH 4. Glu267 does not show any sign of disorder on the basis of its thermal factor, which is comparable to the average *B* value of the protein atoms. While a water molecule was found near the original position of Glu267 OE2 at pH 4, it is not present in the apo structure. This may possibly be due to the lower-resolution data of the apotoxin structure. There is a water molecule near the original zinc atom position (~1.4 Å away). This water molecule makes hydrogen bonds with His229 NE2 and His233 NE2 with distances 3.57 and 3.0 Å, respectively, but makes no hydrogen bond contacts with Glu230. The density for this water molecule appears to be elongated, and it could be disordered and might partially occupy the position corresponding to the original nucleophilic water molecule (Figure 1).

Role of Zinc in Botulinum Neurotoxins. The role of zinc in proteins could be either structural, functional, or both. In general, a catalytic zinc is coordinated to three amino acid residues and an activated water molecule (nucleophilic water). A structural zinc will be coordinated to four amino acid residues (*16*, *17*). In botulinum neurotoxins, classified

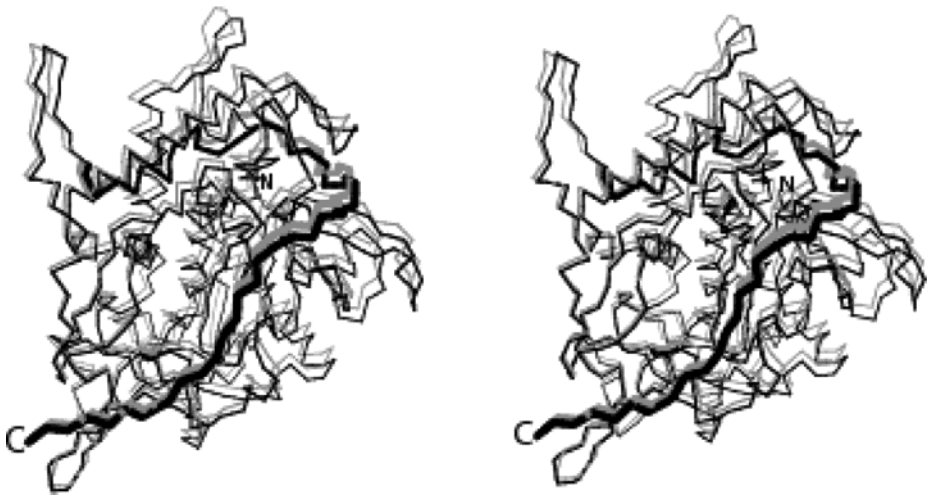

FIGURE 6: Superposition of α-C chains at pH 6.0 (gray) and 7.0 (black). The orientation of the belt region remains the same at all pH values and shows that in all cases the active site cavity is exposed and accessible to substrates. The belt region over the cavity is shown in thicker lines than the rest of the molecule.

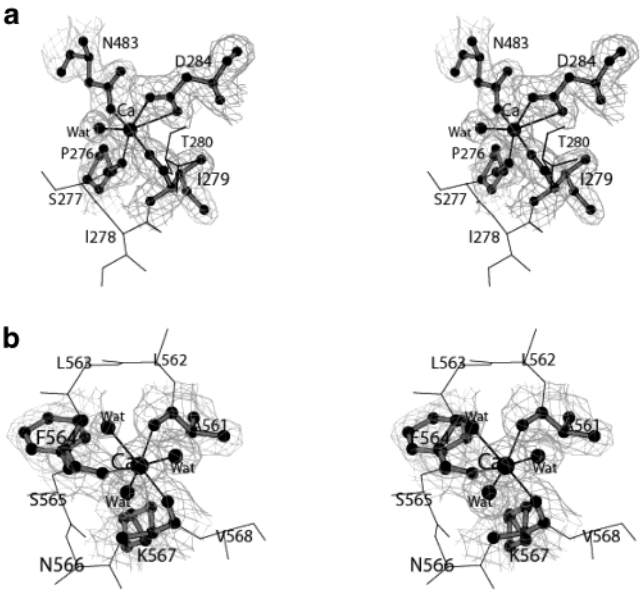

FIGURE 7: SigmaA-weighted $2F_o - F_c$ maps with the final Ca^{2+} positions superimposed: (a) calcium 1293 and (b) calcium 1294. Contours are drawn at the 1σ level.

as gluzincins, the zinc atom is coordinated with three amino acid residues and one water and is thought to be catalytic (*18*). It has been reported that the removal of zinc is reversible in botulinum neurotoxins while the catalytic activity is not. This led to the belief that the tertiary structure of the protein changes irreversibly when the zinc is removed (*21*). However, it has also been shown that zinc-depleted toxins can reach the cytosol and could be active since they could be reconstituted with zinc present in cytosol, which implies that there is no change in the conformation (*23*).

The presumed change in the tertiary structure was studied by biophysical methods (UV circular dichroism in BoNT/A). While no change in the conformation of tyrosine residues was observed, there were indications about the conformational change for phenylalanine residues. In BoNT/B, there are three phenylalanine residues in the light chain (194, 202, and 220). The α-C atoms of these residues are less than 16 Å from the zinc atom, but no change in their conformation or solvent accessibility is seen in either the holotoxin at pH 4.0 or apotoxin. However, for the BoNT/A light chain, the activity is reported to be partly restored when the protein is reconstituted with zinc. There are other reports which also suggest that the activity is restored. From our structural studies on the apotoxin, it is clear that removal of zinc does not affect the stability or conformation of the protein, and it could be concluded that its role is catalytic rather than structural. A similar role for active site zinc has also been proposed in carboxypeptidase (*45*).

Calcium Ions in Botulinum Neurotoxins. During the course of the high-resolution structural analysis, an interesting feature was discovered. Two strong peaks in the electron density map were observed which could not be ascribed to water molecules because of the relative peak heights and the comparatively short distance to the surrounding oxygens. They were identified as calcium ions and refined accordingly (Figure 7). The $F_o - F_c$ map with these two calcium ions included in the refinement showed no residual peak. One calcium ion is predominantly coordinated by light chain residues. It is coordinated by Pro276 O, Ile279 O, Asp284 OD1, Asp284 OD2, Asn483 ND2, and a water molecule (Table 2). While residues 276, 279, and 284 belong to the light chain, residue 483 belongs to the translocation domain and is in the beginning of the belt region. It is a slightly distorted octahedral coordination. The second calcium ion is entirely coordinated by the translocation domain and water molecules. It is coordinated by Ala561 O, Phe564 O, Lys567 O, and three water molecules which form a perfect octahedron (Figure 8 and Table 2). The coordination distances are in the range of 2.2−2.4 Å, values characteristic of calcium−oxygen contacts observed in calcium-containing

Table 2: Calcium Ion Coordination Distances

calcium	protein ligand	distance (Å)	calcium	protein ligand	distance (Å)
Ca 1293	Asp284 OD1	2.29	Ca 1294	Ala561 O	2.22
	Asp284 OD2	2.99		Phe564 O	2.24
	Pro276 O	2.39		Lys567 O	2.18
	Ile279 O	2.24		water 1349 O	2.18
	Asn483 ND2	2.26		water 1368 O	2.21
	water 1720 O	2.75		water 2018 O	2.41

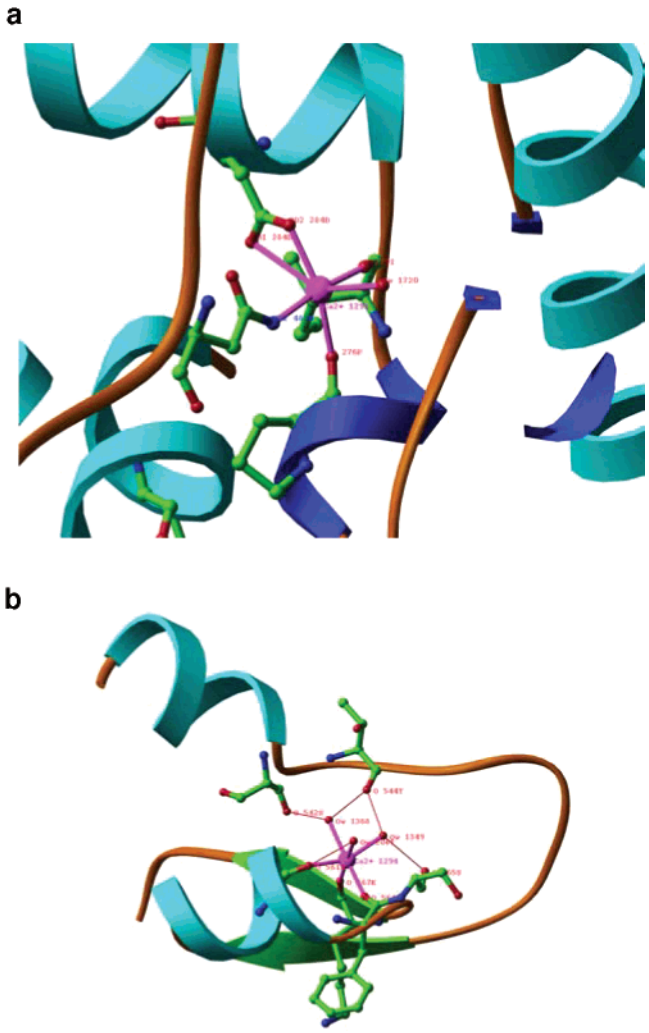

FIGURE 8: Coordination of calcium ions shown along with the secondary structure. (a) Calcium 1293 coordinates with Pro276, Ile279, Asp284, Asn483, and a water molecule and links the light chain and the belt region. This calcium ion may play a role in the translocation. (b) Calcium 1294 coordinates with Ala561, Phe564, Lys567, and three water molecules and is completely coordinated by residues in the translocation domain. This figure was prepared with Ribbons (*53*).

proteins (*46*−*48*). These interactions stabilize a knotlike loop (helix−β−helix). Ala561 and Lys567 (except in BoNT/A where it is Arg, a similarly charged residue) are conserved in all botulinum toxins and tetanus toxin. However, the coordination is through main chain oxygen atoms only. The two calcium ions have solvent accessibilities of 5 and 13 Å^2, and are almost buried.

Interestingly, in most of the zinc endopeptidases, calcium ions are present in addition to zinc. In thermolysin, four calcium ions are present and the thermal stability is attributed to these calcium ions (*48*, *49*). A calcium ion has also been identified in zinc endopeptidase adamalysin II and is thought to be important for structural stability (*47*). Calcium ions have not been identified so far in botulinum toxins by biochemical methods. However, in the initial spectroscopic experiments, only Zn, Co, Cu, Fe, Mn, and Ni were tested, not calcium. The activity of the zinc-depleted BoNT/A LC could be restored to ~20−30% of its original level by adding a divalent metal such as Mn, Mg, or Ca (*50*). Because of the nature of the binding site, it may have some functional role in addition to a structural role.

In the structures determined at various pHs, the calcium ions are intact and are not removed like zinc. This may be because the coordinating atoms are mostly main chain oxygens which are not protonated even at pH 3.0. However, in the apotoxin structure where the toxin was incubated with EDTA before crystallization, the two calcium ions are removed and are replaced with water molecules and the coordinating distances are increased to hydrogen bonding distances. The original calcium sites are perturbed, but no major change in the main chain fold is observed.

Role of Ca^{2+} in Biological Function. It is unknown if Ca^{2+} has a direct role in the biological activity of BoNTs. Ca^{2+} is not needed for catalytic activity, which proceeds unimpeded when BoNT was incubated with BAPTA prior to mixing with the solubilized SNAP-25 substrate (Figure 2a). To test the effect of Ca^{2+} on the catalytic activity of each serotype, BoNTs were added to neuronal cell lysates in the presence or absence of BAPTA or the zinc-specific chelator TPEN (*51*). BAPTA had no effect on the catalytic activity of either toxin (Figure 2a), whereas TPEN totally inhibited both BoNTs. We conclude that the two Ca^{2+} atoms do not influence light chain activity. To test if Ca^{2+} participates in the entry of toxin into cells, BoNT was applied to cultured neurons followed by the membrane-permeable BAPTA-AM or TPEN. These chelators were chosen because both are membrane-permeable, allowing both to act on intracellular BoNT. The amount of BoNT applied to cells was previously determined to cut approximately half of the total SNAP-25 or VAMP. BAPTA-AM effectively protected SNAP-25 and VAMP from BoNT/A and -B, respectively (Figure 2b). Furthermore, addition of Ca^{2+} 1 h after addition of either toxin restored BoNT activity, indicating that BAPTA-AM inhibits BoNT by removing Ca^{2+} (Figure 2c). Only a low-resolution crystal structure of BoNT/A is available, and accordingly, water molecules and other possible ions (except the active site zinc) have not been modeled. On the basis of the sequence homology and structural similarity of BoNT/A and BoNT/B, calcium ions will be present in BoNT/A and other *Clostridium* neurotoxins. Also, the coordination to calcium ion is mostly from main chain oxygen atoms in BoNT/B. A structural alignment of BoNT/A and -B reveals similar sequence homology at the calcium sites. Moreover, the electrostatic charge distribution is similar in BoNT/A and -B at the calcium site (data not shown).

Therefore, the results in living cells in combination with the cell-free SNARE cleavage assay demonstrate that neither Ca^{2+} atom contributes to catalytic activity but at least one Ca^{2+} atom is required for uptake of the toxin into neurons. Because addition of excess Ca^{2+} after toxin exposure reverses the BAPTA-AM effect in living cells, we presume Ca^{2+} is required for toxin activity after toxin uptake but before SNARE damage. Because Ca^{2+} is not required for toxin catalytic activity, we hypothesize that the Ca^{2+} atom coordinated by the light and heavy chains is required for either channel formation or LC translocation through the channel. The Ca^{2+} might allow the light chain to separate or change conformation as it enters the cytosol.

ACKNOWLEDGMENT

We thank Drs. A. Saxena and M. Becker for providing us beam time on the X12C and X25 beamlines of the National Synchrotron Light Source.

REFERENCES

1. Montecucco, C., and Schiavo, G. (1995) Structure and function of tetanus and botulinum neurotoxins, *Q. Rev. Biophys. 28*, 423−472.
2. Simpson, L. L. (1986) Molecular pharmacology of botulinum toxin and tetanus toxin, *Annu. Rev. Pharmacol. Toxicol. 26*, 427−453.
3. Schiavo, G., Matteoli, M., and Montecucco, C. (2000) Neurotoxins affecting neuroexocytosis, *Physiol. Rev. 80*, 717−766.
4. Schantz, E. J., and Johnson, E. A. (1992) Properties and use of botulinum toxin and other microbial neurotoxins in medicine, *Microbiol. Rev. 56*, 80−99.
5. Menestrina, G., Schiavo, G., and Montecucco, C. (1994) Molecular mechanisms of action of bacterial protein toxins, *Mol. Aspects Med. 15*, 79−193.
6. Oguma, K., Fujinaga, Y., and Inoue, K. (1995) Structure and Function of *Clostridium botulinum* toxins, *Microbiol. Immunol. 39*, 161−168.
7. Schiavo, G., Rossetto, O., Santucci, A., Dasgupta, B. R., and Montecucco, C. (1992) Botulinum neurotoxins are zinc proteins, *J. Biol. Chem. 267*, 23479−27483.
8. Blasi, J., Chapman, E. R., Link, E., Binz, T., Yamasaki, S., Camilli, P. D., Sudhof, T. C., Niemann, H., and Jahn, R. (1993) Botulinum neurotoxin A selectively cleaves the synaptic protein SNAP-25, *Nature 365*, 160−163.
9. Blasi, J., Chapman, E. R., Yamasaki, S., Binz, T., Niemann, H., and Jahn, R. (1993) Botulinum neurotoxin C blocks neurotransmitter release by means of cleaving HPC-1/syntaxin, *EMBO J. 12*, 4821−4828.
10. Binz, T., Blasi, J., Yamasaki, S., Baumeister, A., Link, E., Sudhof, T. C., Jahn, R., and Niemann, H. (1994) Proteolysis of SNAP-25 by Types E and A botulinum neurotoxins, *J. Biol. Chem. 269*, 1617−1620.
11. Schiavo, G., Shone, C. C., Rossetto, O., Alexander, F. C. G., and Montecucco, C. (1993) Botulinum neurotoxin serotype F is a zinc endopeptidase specific for VAMP/synaptobrevin, *J. Biol. Chem. 268*, 11516−11519.
12. Schiavo, G., Santucci, A., Dasgupta, B. R., Metha, P. P., Jontes, J., Benfenati, F., Wilson, M. C., and Montecucco, C. (1993) Botulinum neurotoxins serotypes A and E cleave SNAP-25 at distinct COOH-terminal peptide bonds, *FEBS Lett. 335*, 99−103.
13. Schiavo, G., Malizio, C., Trimble, W. S., Polverino-de-Laureto, P., Milan, G., Sugiyama, H., Johnson, E. A., and Montecucco, C. (1994) Botulinum G neurotoxin cleaves VAMP/synaptobrevin at a single Ala-Ala peptide bond, *J. Biol. Chem. 269*, 20213−20216.
14. Schiavo, G., Benfenati, F., Poulain, B., Rossetto, O., de-Lauretto, P. P., Dasgupta, B. R., and Montecucco, C. (1992) Tetanus and botulinum-B neurotoxins block neurotransmitter release by a proteolytic cleavage of synaptobrevin, *Nature 359*, 832−835.

15. Schiavo, G., Shone, C. C., Bennett, M. K., Scheller, R. H., and Montecucco, C. (1995) Botulinum neurotoxin type C cleaves a single Lys-Ala bond within the carboxyl-terminal region of syntaxins, *J. Biol. Chem. 270*, 10566−10570.
16. Vallee, B. L., and Auld, D. S. (1990) Zinc coordination, function, and structure of zinc enzymes and other proteins, *Biochemistry 29*, 5647−5659.
17. Vallee, B. L., and Auld, D. S. (1990) Active-site zinc ligands and activated H_2O of zinc enzymes, *Proc. Natl. Acad. Sci. U.S.A. 87*, 220−224.
18. Hooper, N. M. (1994) Families of zinc metalloproteases, *FEBS Lett. 354*, 1−6.
19. Foran, P., Shone, C. C., and Dolly, J. O. (1994) Differences in the protease activities of tetanus and botulinum B toxins revealed by the cleavage of vesicle-associated membrane protein and various sized fragments, *Biochemistry 33*, 15365−15374.
20. Fillippis, V. D., Vangelista, L., Schiavo, G., Tonello, F., and Montecucco, C. (1995) Structural studies on the zinc-endopeptidase light chain of tetanus neurotoxin, *Eur. J. Biochem. 229*, 61−69.
21. Fu, F., Lomneth, R. B., Cai, S., and Singh, B. R. (1998) Role of zinc in the structure and toxic activity of botulinum neurotoxin, *Biochemistry 37*, 5267−5278.
22. Li, L., and Singh, B. R. (2000) Role of zinc binding in type A botulinum neurotoxin light chain's toxic structure, *Biochemistry 39*, 10581−10586.
23. Simpson, L. L., Maksymowych, A. B., and Hao, S. (2001) The role of zinc binding in the biological activity of botulinum toxin, *J. Biol. Chem. 276*, 27034−27041.
24. Montecucco, C., Papini, E., and Schiavo, G. (1994) Bacterial protein toxins penetrate cells via a four-step mechanism, *FEBS Lett. 346*, 92−98.
25. Koriazova, L., and Montal, M. (2003) Translocation of botulinum neurotoxin light chain protease through the heavy chain channel, *Nat. Struct. Biol. 10*, 13−18.
26. Kadkhodayan, S., Knapp, M. S., Schmidt, J. J., Fabes, S. E., Rupp, B., and Balhorn, R. (2000) Cloning, expression, and one-step purification of the minimal essential domain of the light chain of botulinum neurotoxin type A, *Protein Expression Purif. 19*, 125−130.
27. Ransom, B. R., Neale, E., Henkart, M., Bullock, P. N., and Nelson, P. G. (1977) Mouse spinal cord in cell culture. I. Morphology and intrinsic neuronal electrophysiologic properties, *J. Neurophysiol. 40*, 1132−1150.
28. Fitzgerald, S. C. (1989) in *A Dissection and Tissue Culture Manual of the Nervous System* (Sharar, A., Devellis, J., Vernadakis, A., and Javer, B., Eds.) pp 219−222, Alan R. Liss, Inc., New York.
29. Williamson, L. C., Fitzgerald, S. C., and Neale, E. A. (1992) Differential effects of tetanus toxin on inhibitory and excitatory neurotransmitter release from mammalian spinal cord cells in culture, *J. Neurochem. 59*, 2148−2157.
30. Laemmli, U. K. (1970) Cleavage of structural proteins during the assembly of the head of bacteriophage T4, *Nature 227*, 680−685.
31. Li, L., Binz, T., Niemann, H., and Singh, B. R. (2000) Probing the mechanistic role of glutamate residues in the zinc-binding motif of type A botulinum neurotoxin light chain, *Biochemistry 39*, 2399−2405.
32. Swaminathan, S., and Eswaramoorthy, S. (2000) Structural analysis of the catalytic and binding sites of *Clostridium botulinum* neurotoxin B, *Nat. Struct. Biol. 7*, 693−699.
33. Swaminathan, S., and Eswaramoorthy, S. (2000) Crystallization and preliminary X-ray analysis of *Clostridium botulinum* neurotoxin type B, *Acta Crystallogr. D56*, 1024−1026.
34. Otwinowski, Z., and Minor, W. (1997) Processing of X-ray diffraction data collected in oscillation mode, *Methods Enzymol. 276*, 307−326.
35. Brunger, A. T., Adams, P. D., Clore, G. M., Delano, W. L., Gros, P., Grosse-Kunstleve, R. W., Jiang, J. S., Kuszwewski, J., Nilges, M., Pannu, N. S., Read, R. J., Rice, L. M., Somonsom, T., and Warren, G. L. (1998) Crystallography and NMR system: a new software suite for macromolecular structure determination, *Acta Crystallogr. D54*, 905−921.
36. Jones, T. A., Zou, J., Cowtan, S., and Kjeldgaard, M. (1991) Improved methods in building protein models in electron density map and the location of errors in these models, *Acta Crystallogr. A47*, 110−119.
37. Furey, W., and Swaminathan, S. (1997) PHASES-95: A program package for the processing and analysis of diffraction data from macromolecules, *Methods Enzymol. 276*, 590−620.
38. Laskowski, R. A., MacArthur, M. W., Moss, D. S., and Thornton, J. M. (1993) PROCHECK: a program to check the stereochemical quality for assessing the accuracy of protein structures, *J. Appl. Crystallogr. 26*, 283−291.
39. Hoch, D. H., Romero-Mira, M., Ehrlich, B. E., Finkelstein, A., DasGupta, B. R., and Simpson, L. L. (1985) Channels formed by botulinum, tetanus, and diphtheria toxins in planar lipid bilayers: relevance to translocation of proteins across membranes, *Proc. Natl. Acad. Sci. U.S.A. 82*, 1692−1696.
40. Overly, C. C., Lee, K. D., Berthiaume, E., and Hollenbeck, P. J. (1995) Quantitative measurement of intraorganelle pH in the endosomal-lysosomal pathway in neurons by using ratiometric imaging with pyranine, *Proc. Natl. Acad. Sci. U.S.A. 92*, 3156−3160.
41. Persson, B., and Argos, P. (1996) Topology prediction of membrane proteins, *Protein Sci. 5*, 363−371.
42. Lacy, D. B., Tepp, W., Cohen, A. C., DasGupta, B. R., and Stevens, R. C. (1998) Crystal structure of botulinum neurotoxin type A and implications for toxicity, *Nat. Struct. Biol. 5*, 898−902.
43. Bullough, P. A., Hughson, F. M., Skehel, J. J., and Wiley, D. C. (1994) Structure of influenza haemagglutinin at the pH of membrane fusion, *Nature 371*, 37−43.
44. Li, L., and Singh, B. R. (2000) Spectroscopic analysis of pH-induced changes in the molecular features of type A botulinum neurotoxin light chain, *Biochemistry 39*, 6466−6474.
45. Greenblatt, H. M., Feinberg, H., Tucker, P. A., and Shoham, G. (1998) Carboxypeptidase A: Native, zinc-removed and mercury-replaced forms, *Acta Crystallogr. D54*, 289−305.
46. Bode, W., and Schwager, P. (1975) The refined crystal structure of bovine beta-trypsin at 1.8 Å resolution. II. Crystallographic refinement, calcium binding site, benzamidine binding site and active site at pH 7.0, *J. Mol. Biol. 98*, 693−717.
47. Gomis-Ruth, F. X., Kress, L. F., Kellermann, J., Mayr, I., Lee, X., Huber, R., and Bode, W. (1994) Refined 2.0 Å X-ray structure of the snake venom zinc endopeptidase adamalysin II, *J. Mol. Biol. 239*, 513−544.
48. Colman, P. M., Jansonius, J. N., and Matthews, B. W. (1972) The structure of thermolysin: an electron density map at 2−3 Å resolution, *J. Mol. Biol. 70*, 701−724.
49. Matthews, B. W., Weaver, L. H., and Kester, W. R. (1974) The conformation of thermolysin, *J. Biol. Chem. 249*, 8030−8044.
50. Ahmed, S. A., and Smith, L. A. (2000) Light chain of botulinum A neurotoxin expressed as an inclusion body from a synthetic gene is catalytically and functionally active, *J. Protein Chem. 19*, 475−487.
51. Simpson, L. L., Coffield, J. A., and Bakry, N. (1993) Chelation of zinc antagonizes the neuromuscular blocking properties of the seven serotypes of botulinum neurotoxin as well as tetanus toxin, *J. Pharmacol. Exp. Ther. 267*, 720−727.
52. Kraulis, P. J. (1991) MOLSCRIPT: a program to produce both detailed and schematic plots of proteins, *J. Appl. Crystallogr. 24*, 946−950.
53. Carson, M. (1991) Ribbons 2.0, *J. Appl. Crystallogr. 24*, 958−961.

BI035844K